Available online at www.sciencedirect.com
ScienceDirect
Dyes and Pigments 76 (2008) 706–713
DYES and PIGMENTS
www.elsevier.com/locate/dyepig

Titanium dioxide-mediated photocatalytic degradation of Acridine Orange in aqueous suspensions under UV irradiation

Chung-Shin Lu [a], Fu-Der Mai [b], Chia-Wei Wu [b], Ren-Jang Wu [c], Chiing-Chang Chen [a,*]

[a] *Department of General Education, National Taichung Nursing College, No. 193, Sec. 1, San-Min Road, Taichung 403, Taiwan, ROC*
[b] *Department of Applied Chemistry, Chung-Shan Medical University, Taichung 402, Taiwan, ROC*
[c] *Department of Applied Chemistry, Providence University, Taichung 433, Taiwan, ROC*

Received 10 November 2006; received in revised form 18 January 2007; accepted 19 January 2007
Available online 30 January 2007

Abstract

The TiO_2/UV photocatalytic degradation of Acridine Orange (AO) was investigated in aqueous heterogeneous suspension. The results indicated that photocatalytic reactions were enhanced in alkaline medium. While the rate of photocatalytic degradation of the dye increased with increasing concentration of TiO_2, at high doses of TiO_2, the rate of reaction was reduced as a result of light attenuation. To obtain a better understanding of the mechanistic details of this TiO_2 assisted dye photodegradation, the intermediates of the processes were separated, identified, and characterized using HPLC–ESI-MS. It was found that *N*-de-methylation degradation of the dye took place in a stepwise manner to yield mono-, di-, tri-, and tetra-*N*-de-methylated species. The probable photodegradation pathways are proposed and discussed.

Keywords: Titanium dioxide; Acridine Orange; Dye; *N*-De-methylation

1. Introduction

Acridine Orange (AO) is a heterocyclic dye containing nitrogen atoms which is widely used in the field of printing and dyeing, leather, printing ink and lithography [1]; the dye is also used extensively in biological staining. Toxicological investigations indicate that aminoacridine has mutagenic potential [2]; it is a serious pollutant in wastewater and difficult to treat by common removal methods such as coagulation and biodegradation, but few studies on its treatment have appeared. The release of wastewater containing the dye poses a dramatic source of water pollution, eutrophication and perturbation of aquatic life [3]. Therefore, a method of treating wastewater containing AO is highly desirable.

To de-pollute dye wastewater, several methods have been investigated, including chemical oxidation and reduction, chemical precipitation and flocculation, photolysis, adsorption, ion pair extraction, electrochemical treatment and advanced oxidation [4]. Advanced oxidation is one of the most promising technologies for the removal of dye-contaminated wastewater due to its high efficiency. It is based mainly on the oxidative reactivity of $HO^{\bullet}$ radicals generated by various methods such as O_3/UV, H_2O_2/UV, H_2O_2/Vis, O_3/H_2O_2/UV photolysis, photoassisted Fe^{3+}/H_2O_2, and TiO_2-mediated photocatalysis processes. Since pollutants could be completely degraded to harmless compounds by photocatalysis under normal temperature and air pressure, it is predicted that photocatalysis will soon become one of the most effective means of dealing with various kinds of industrial wastewater [5].

The TiO_2-mediated photocatalysis process has been successfully used to degrade pollutants in recent years [6–13]. TiO_2 is used as a photocatalyst because of its nontoxicity, photochemical stability and low cost [14,15]. The initial step in TiO_2-mediated photocatalysis involves the generation of an

* Corresponding author. Tel.: +886 4 2219 6973; fax: +886 4 2219 4990.
E-mail addresses: cslu6@ntcnc.edu.tw (C.-S. Lu), ccchen@ntcnc.edu.tw (C.-C. Chen).

0143-7208/$ - see front matter © 2007 Elsevier Ltd. All rights reserved.
doi:10.1016/j.dyepig.2007.01.009

(e^-/h^+) pair, leading to the formation of hydroxyl radicals ($^{\bullet}OH$), superoxide radical anions ($O_2^{\bullet-}$), and hydroperoxyl radicals ($^{\bullet}OOH$) as shown below [16–18]:

$$TiO_2 + h\nu \rightarrow TiO_2(h^+ + e^-) \quad (1)$$

$$H_2O_{(ads)} + h^+ \rightarrow {}^{\bullet}OH + H^+ \quad (2)$$

$$OH^- + h^+ \rightarrow {}^{\bullet}OH \quad (3)$$

$$O_2 + e^- \rightarrow O_2^{\bullet-} \quad (4)$$

$$O_{2(ads)} + e^- + H^+ \rightarrow HO_2^{\bullet} \quad (5)$$

Organic pollutants are attacked and oxidized by the radicals formed through the above mechanisms. In addition to hydroxyl radicals, superoxide radical anions—and in some cases the positive holes—are also suggested as possible oxidizing species that can attack organic contaminants present at or near the surface of TiO_2 [19].

Little has been reported on the degradation of AO under UV light in the presence of TiO_2. Muneer et al. [3] investigated the photocatalytic degradation of AO and ethidium bromide in aqueous suspensions of TiO_2; degradation rates were found to be strongly influenced by the operation parameters. Ma et al. [20] reported a photocatalyst of TiO_2/γ-Fe_2O_3 that can photodegraded AO in dispersion while Gao and Liu [21] investigated the photodegradation of AO and phenol in aqueous solution using a suspended photocatalyst of TiO_2-activated carbon immobilized on silicone rubber film. In all of these studies, photocatalytic degradation was monitored using UV spectroscopy.

Although the TiO_2/UV photocatalytic degradation kinetics in the context of AO have been studied in the past, the photodegradation intermediates of this dye have not been isolated or identified. Only very limited information on the photocatalytic intermediates and reaction mechanisms is available. In this paper, the reaction intermediates were identified using HPLC–ESI-MS, which enabled the degradation mechanism and reaction pathways of the photodegradation of AO in TiO_2/UV to be identified.

2. Experimental section

2.1. Materials

TiO_2 nanoparticles (P25, ca. 80% anatase, 20% rutile; particle size, ca. 20–30 nm; BET area, ca. 55 $m^2\,g^{-1}$) were supplied by Degussa. Acridine Orange (Fig. 1) and 3,6-diaminoacridine were obtained from Sigma–Aldrich and used without further purification. Stock solutions containing 1 $g\,L^{-1}$ of dye in water were prepared, protected from light and were stored at 4 °C. HPLC analysis was employed to confirm the presence of the dye as a pure organic compound. Reagent-grade ammonium acetate, sodium hydroxide, nitric acid, and HPLC-grade methanol were purchased from Merck. Deionized water (resistivity of $1.8 \times 10^7\,\Omega\,cm$) purified using a Milli-Q water ion-exchange system (Millipore) was used.

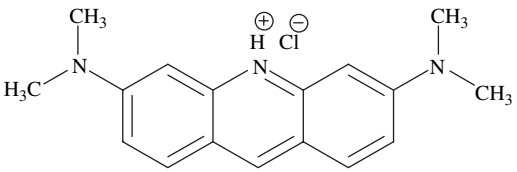

Fig. 1. Chemical structure of Acridine Orange.

2.2. Apparatus and instruments

The apparatus for studying the photocatalytic degradation of AO has been described elsewhere [13]. The C-75 Chromato-Vue cabinet of UVP provides a wide area of illumination from the 15-W UV-365 nm tubes positioned on two sides of the cabinet interior. A Waters ZQ LC/MS system, equipped with a binary pump, a photodiode array detector, an autosampler, and a micromass detector, was used for separation and identification.

2.3. Procedures and analysis

An aqueous TiO_2 dispersion was prepared by adding 50 mg of TiO_2 powder to a 100 mL solution containing the dye at an appropriate concentration. For reactions in different pH media, the initial pH of the suspensions was adjusted by the addition of either aq NaOH or HNO_3 solution. Prior to irradiation, the dispersions were magnetically stirred in the dark for 30 min to ensure the establishment of adsorption/desorption equilibrium. Irradiation was carried out using two UV-365 nm lamps (15 W); at any given irradiation time interval, the dispersion was sampled (5 mL), centrifuged and subsequently filtered through a Millipore filter (pore size, 0.22 μm) to separate the TiO_2 particles.

After each irradiation cycle, the amount of residual dye was determined by HPLC. The analysis of organic intermediates was accomplished by HPLC–ESI-MS after the readjustment of the chromatographic conditions in order to make the mobile phase compatible with the working conditions of the mass spectrometer. Two different kinds of solvents were prepared in this study namely, Solvent A, 25 mM aqueous ammonium acetate buffer (pH 6.9) and solvent B, methanol. LC was carried out on an *Atlantis dC18* column (250 mm × 4.6 mm i.d., dp = 5 μm). The flow rate of the mobile phase was set at 1.0 mL min^{-1}. The chromatographic conditions for gradient elution of AO are shown in Table 1. The column effluent was introduced into the ESI source of the mass spectrometer, which was equipped with an ESI interface, the quadruple mass spectrometer having a heated nebulizer probe at 350 °C that was used with an ion source temperature of 120 °C. ESI was carried out with the vaporizer set at 300 °C, nitrogen as both sheath (80 psi) and auxiliary (20 psi) gas to assist with preliminary nebulization and to initiate the ionization process. A discharge current of 5 μA was used; tube lens and capillary voltages were optimized for the maximum response during perfusion of the AO standard.

Table 1
The chromatographic condition for gradient elution of Acridine Orange

Time (min)	% Solvent A	% Solvent B
0	95	5
20	50	50
35	10	90
40	10	90
45	95	5

3. Results and discussion

3.1. pH effect

Many studies have indicated that the pH of a solution is an important parameter in the photocatalytic degradation of organic compounds due to the fact that pH influences the surface charge of the semiconductor, thereby affecting interfacial electron transfer and, therefore, the photoredox process [22]. The zero point of charge (zpc) of semiconductor particles is defined as the pH at which the concentrations of the protonated and deprotonated groups are equal, i.e., pH zpc = $1/2(pK_1 + pK_2)$. The pH zpc of TiO_2 is 6.25 and so its surface is predominately positively charged below pH zpc (i.e., $Ti\text{-}OH + H^+ \leftrightarrows TiOH_2^+$) and negatively charged above pH zpc (i.e., $Ti\text{-}OH + OH^- \leftrightarrows TiO^- + H_2O$). Thus, the electrical character of the TiO_2 surface varies with the pH of the dispersion [23]. The surface of TiO_2 is negatively charged and adsorbs cationic species readily under pH > pH zpc conditions whilst, under reverse conditions, it adsorbs anionic species. However, the adsorption of the substrate onto the TiO_2 surface directly affects electron transfer between the excited dye and TiO_2, which, in turn, influences the degradation rate. A similar effect of pH on adsorption and photocatalytic reaction has been reported for Ag deposition [24] and the degradation of formic acid [25].

The photodegradation rate of AO as a function of reaction pH is shown in Fig. 2 from which it is evident that the rate of degradation proceeded much faster at alkaline pH values. Under acidic conditions, it was difficult for the cationic dye to adsorb onto the TiO_2 surface. With the active $^{\bullet}OH$ radicals usually in low concentration, the photodegradation of AO occurred slowly. At higher pH values, the formation of active $^{\bullet}OH$ species is favoured, not only because of improved transfer of holes to the adsorbed hydroxyls, but also due to electrostatic attractive effects operating between the negatively charged TiO_2 particles and the cationic dye.

3.2. Effect of TiO_2 dosage

It is important from both the mechanistic and application points of view to study the dependence of the photocatalytic reaction rate on the concentration of TiO_2. Hence, the effect of TiO_2 dosage on the photodegradation rate of the dye was investigated by employing different concentrations of TiO_2 varying from 0.1 to 3.0 g L^{-1}. While the photocatalytic degradation rate was found to increase with increasing TiO_2 dosage, the reaction was retarded at high TiO_2 dosages (Fig. 3). The increase in rate was likely due to the increase in the total surface area (or number of active sites) available for photocatalytic reaction as the dosage of TiO_2 increased. However, at very high TiO_2 dosage, the intensity of the incident UV light was attenuated because of reduced light penetration and increased light scattering [26].

3.3. Effect of dye concentration

When the initial dye concentration was varied from 0.05 to 0.25 g L^{-1} at constant TiO_2 dosage (0.5 g L^{-1}, pH 6), Fig. 4 shows that degradation efficiency was inversely affected by dye concentration. This can be explained as follows: as the dye concentration increased, the equilibrium adsorption of the dye on the catalyst surface increased, and, thereby the competitive adsorption of OH^- on the same adsorption sites decreased, resulting in a lower rate of formation of $^{\bullet}OH$ radical, the principal oxidant necessary for high degradation efficiency. In contrast, considering the Beer–Lambert law, as the initial dye concentration increased, the path length of the photons entering the solution decreased, resulting in lower photon absorption on catalyst particles and, consequently, lower photodegradation rate.

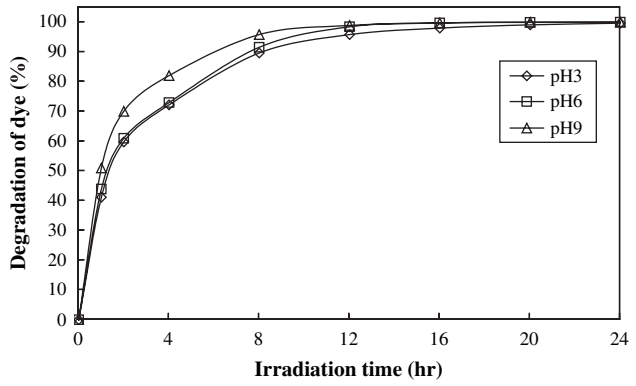

Fig. 2. pH effect on the AO photodegradation rate with concentrations of TiO_2 at 0.5 g L^{-1} and AO at 0.05 g L^{-1}: (a) pH 3; (b) pH 6; (c) pH 9.

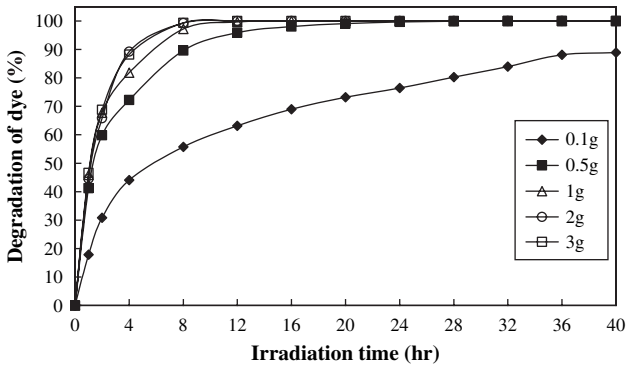

Fig. 3. Effect of TiO_2 dosage on the photodegradation rate for the decomposition of AO. Experimental conditions: dye concentration (0.05 g L^{-1}), at pH 6, absorbance was recorded at 492 nm, continuous stirring, irradiation time 40 h.

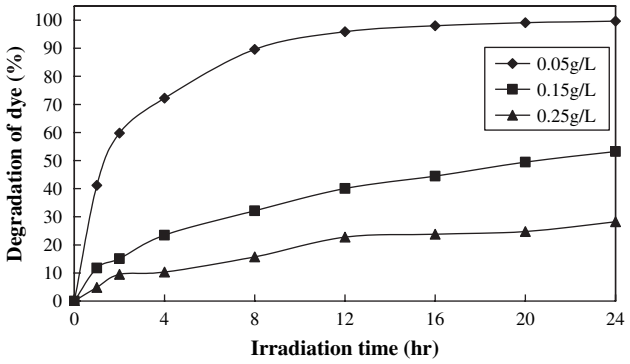

Fig. 4. Effect of initial dye concentration on the photodegradation rate for the decomposition of AO.

3.4. UV-visible spectra

AO can be degraded efficiently in aqueous AO/TiO_2 dispersions by UV irradiation at wavelength 365 nm. The changes of the UV-visible spectra during the photodegradation process of the AO dye are illustrated in Fig. 5. About 99.7% of the dye was degraded after irradiation for 24 h. The characteristic absorption band of the dye at around 492 nm decreased rapidly with slight hypsochromic shifts (478 nm), but no new absorption bands appeared even in the UV range ($200\,nm < \lambda < 400\,nm$), which indicated that a series of *N*-de-methylated intermediates may have formed and that the chromophore structure of the AO dye may have been cleaved.

3.5. Separation and identification of the intermediates

Using a relatively low intensity UV-365 nm lamp (15 W) enabled us to obtain slower degradation rates and provide favourable conditions for the determination of intermediates; an initial AO concentration of 0.05 g L^{-1} was selected. This part of the work focused on the identification of the major aromatic intermediates rather than by-products derived from cleavage of the aromatic ring.

Temporal variations occurring in the dye during photodegradation were examined using HPLC, coupled with a photodiode array detector and electrospray ionization mass spectrometry. The chromatograms recorded at 492 nm are illustrated in Fig. 6. With irradiation up to 16 h, six components were identified, all with retention times < 50 min. The dye and its related intermediates are labelled as species **A**–**F**. Except for the initial dye (peak A), the intensities of the other peaks increased at first and subsequently decreased, indicating the formation and transformation of the intermediates. The absorption spectra of each intermediate in the visible region are depicted in Fig. 7. The absorption maximum of the spectral bands shifted hypsochromically from 492.0 (Fig. 7, spectrum A) to 460.5 nm (Fig. 7, Spectrum F). This hypsochromic shift was presumed to result from the stepwise formation of a series of *N*-de-methylated intermediates (i.e., methyl groups were removed one by one as confirmed by the gradual peak wavelength shifts toward the blue region). Similar phenomena were also observed during the photodegradation of rhodamine-B [27,28] and sulforhodamine-B [29–31] under visible irradiation.

The *N*-de-methylated intermediates were further identified using HPLC–ESI-MS (Fig. 8). The molecular ion peaks appeared to be the acid form of the intermediates. From the results of mass spectral analysis, we confirmed that component **A**, $m/z = 266.12$, in the liquid chromatogram was AO (Fig. 8, mass spectrum A). The other components were **B**,

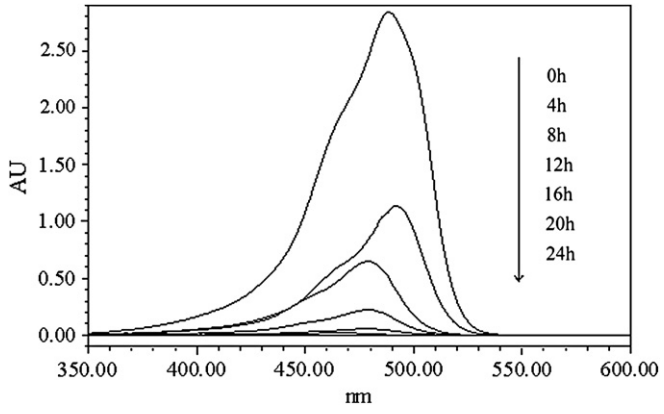

Fig. 5. UV-visible spectra changes of the AO dye in aqueous TiO_2 dispersions (AO 0.05 g L^{-1}, TiO_2 0.5 g L^{-1}) as a function of irradiation time.

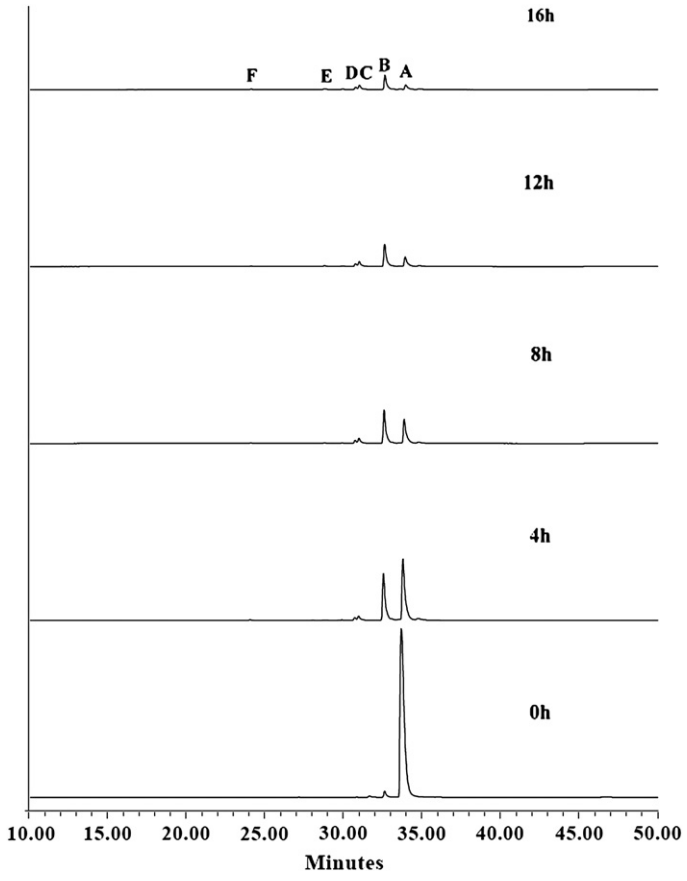

Fig. 6. HPLC chromatograms of the *N*-de-methylated intermediates at different irradiation intervals, recorded at 492 nm. Chromatograms from bottom to top correspond to the irradiation times of 0, 4, 8, 12 and 16 h, respectively.

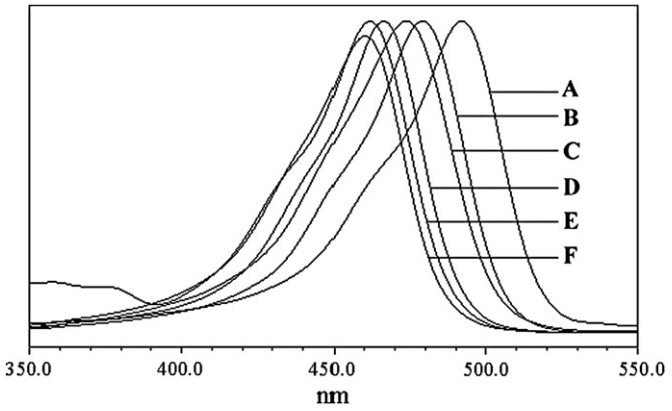

Fig. 7. Absorption spectra of the *N*-de-methylated intermediates formed during the photodegradation process of the AO dye corresponding to the peaks in the HPLC chromatogram of Fig. 6. Spectra were recorded using the photodiode array detector. Spectra A–F correspond to peaks **A**–**F** in Fig. 6, respectively.

$m/z = 252.13$, *N*-de-mono-methyl-Acridine Orange (Fig. 8, mass spectrum B); **C**, $m/z = 238.08$, *N*,*N*′-de-dimethyl-Acridine Orange (Fig. 8, mass spectrum C); **D**, $m/z = 238.14$, *N*,*N*-de-dimethyl-Acridine Orange (Fig. 8, mass spectrum D); **E**, $m/z = 224.09$, *N*,*N*,*N*′-de-trimethyl-Acridine Orange (Fig. 8, mass spectrum E); and **F**, $m/z = 210.04$, *N*,*N*,*N*′,*N*′-de-tetramethyl-Acridine Orange (Fig. 8, mass spectrum F). Table 2 presents the absorption maximum and mass peaks of the *N*-de-methylated intermediates and the corresponding compounds identified by interpretation of their mass spectra. When the proposed *N*-tetra-de-methylated intermediate (AO-DD) was compared with 3,6-diaminoacridine, the retention times and absorption spectra were identical.

According to the number of the methyl groups detached, we can characterize these intermediates. One pair of isomeric molecules, i.e., di-*N*-de-methylated AO species, differed only in their manner of loosening the methyl groups from the amino groups. One of these, AO-MM, was formed by the removal of a methyl group from two different amino groups of the AO molecule. The cleavage of two methyl groups from the same amino group of the AO dye produced the other species, AO-D. Therefore, considering that the polarity of the AO-D species is greater than that of the AO-MM intermediate, we expected the latter to be eluted after the AO-D species. In addition, to the extent that two *N*-methyl groups are stronger auxochromic moieties than either *N*,*N*-dimethyl or amino

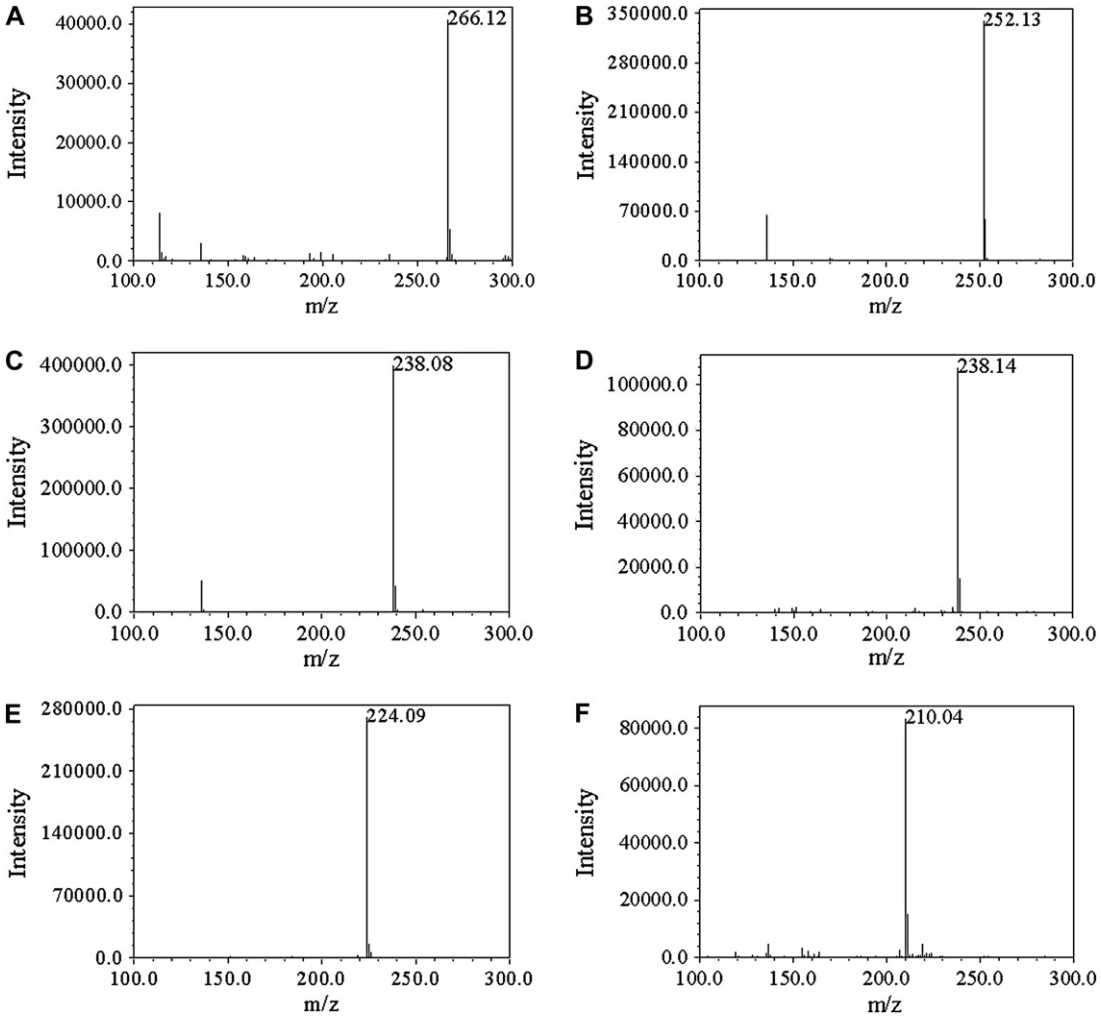

Fig. 8. ESI mass spectra of *N*-de-methylated intermediates formed during the photodegradation of the AO dye after they were separated by HPLC–ESI-MS method. Spectra are denoted A–F and correspond to the **A**–**F** species in Fig. 6, respectively.

Table 2
Identification of the *N*-de-methylation intermediates of the AO dye by HPLC–ESI-MS

HPLC peaks	*N*-De-methylation intermediates	Abbreviation	ESI-MS peaks (*m*/*z*)	Absorption maximum (nm)
A	Acridine Orange	AO	266.12	492.0
B	*N*-de-mono-methyl-Acridine Orange	AO-M	252.13	479.9
C	*N*,*N*′-de-dimethyl-Acridine Orange	AO-MM	238.08	473.8
D	*N*,*N*-de-dimethyl-Acridine Orange	AO-D	238.14	466.5
E	*N*,*N*,*N*′-de-trimethyl-Acridine Orange	AO-DM	224.09	461.7
F	*N*,*N*,*N*′,*N*′-de-tetramethyl-Acridine Orange	AO-DD	210.04	460.5

groups, the maximal absorption of the AO-D intermediate was anticipated to occur at a wavelength shorter than the band position of the AO-MM species.

The relative distribution of the *N*-de-methylated intermediates obtained is illustrated in Fig. 9. By describing the typical bell-shaped profiles, we clearly observed the change in the distribution of each intermediate during the photocatalytic degradation of AO dye. To minimize errors, the relative intensities were recorded at the maximum absorption wavelength for each intermediate. A quantitative determination of all of the photogenerated intermediates was unfortunately not achieved, owing to a lack of the appropriate molar extinction coefficients for these intermediates and the related reference standards. The distribution of all of the *N*-de-methylated intermediates was relative to the initial concentration of AO. It is clear that during the first 24 h of photoreaction, the detected intermediates B–F appeared in their maximum amounts. These compounds may be considered major degradation products, originating from *N*-de-methylation of the substrate molecule.

Most aromatic molecules undergo photocatalytic degradation when irradiated in the presence of suitable semiconductors. This occurs through a multistep process involving the attack on the substrate by a radical species, among which the $^{\bullet}$OH radical has been recognized as being the most powerful oxidant [32]. Nakamura and Nakato [33] proposed a mechanism of water oxidation by nucleophilic attack on a surface-trapped hole at a bridged O site (Eqs. (6)–(8)). Murakami et al. [34] reported that when the O–O bond in Ti–O–OH breaks, the hydroxyl radicals can be formed from the bridge OH groups (Eq. (9)).

$$[\mathrm{Ti-O-Ti}]_s + h^+ + \mathrm{H_2O} \rightarrow [\mathrm{Ti-O^{\bullet}HO-Ti}]_s + \mathrm{H^+} \quad (6)$$

$$[\mathrm{Ti-O^{\bullet}HO-Ti}]_s \rightarrow [\mathrm{Ti-O-O-Ti}]_s + \mathrm{H^+} \quad (7)$$

$$[\mathrm{Ti-O-O-Ti}]_s + \mathrm{H_2O} \rightarrow [\mathrm{Ti-O-OH^{\bullet}HO-Ti}]_s \quad (8)$$

$$[\mathrm{Ti-O-OH^{\bullet}HO-Ti}]_s \rightarrow [\mathrm{Ti-O^{\bullet}HO-Ti}]_s + {}^{\bullet}\mathrm{OH} \quad (9)$$

The *N*-de-methylation of AO occurs mostly through the attack of the $^{\bullet}$OH species on the *N*,*N*-dimethyl groups of the dye. Considering that the *N*,*N*-dimethyl group in AO-M is bulkier than the *N*-methyl group in the AO-M molecules, the attack of $^{\bullet}$OH radicals on the *N*-methyl groups should be favoured at the expense of the *N*,*N*-dimethyl groups. In accord with this notion, the HPLC results showed that the AO-D intermediate reached maximal concentration before the AO-MM intermediate. The *N*-di-de-methylated intermediates (AO-MM and AO-D) were clearly observed (Fig. 9, curve C–D) to reach their maximum concentrations after 12- and 8-h irradiation periods, respectively. The *N*-tri-de-methylated intermediate (AO-DM) was clearly seen (Fig. 9, curve E) to reach its maximum concentration after a 20-h irradiation period because the $^{\bullet}$OH radical attacked the *N*-methyl groups of AO-MM and the *N*,*N*-dimethyl group of AO-D. The successive appearance of the maximal quantity of each intermediate indicates that the *N*-de-methylation of AO is a stepwise photochemical process. The chromophoric species was still observed even after irradiation for 32 h, implying that the *N*-de-methylation process predominates, and, that cleavage of the conjugated structure occurs at a somewhat slower rate until all four methyl groups are removed.

According to earlier reports [35–37], most oxidative *N*-de-alkylation processes are preceded by the formation of a nitrogen-centered radical. On the basis of the above experimental results, we tentatively propose the pathway of *N*-de-methylation in Scheme 1. The dye molecule in the AO/TiO_2 system is adsorbed through the positively charged dimethylamino groups and the $^{\bullet}$OH radicals in the TiO_2 particle surface attack the adsorbed dye and subsequent hydrolysis (or deprotonation) yields a nitrogen-centered radical, which is then attacked by molecular oxygen that results, ultimately, in *N*-de-methylation. The mono-*N*-de-methylated dye, AO-M, can also be adsorbed onto the TiO_2 particle surface and be involved in other similar

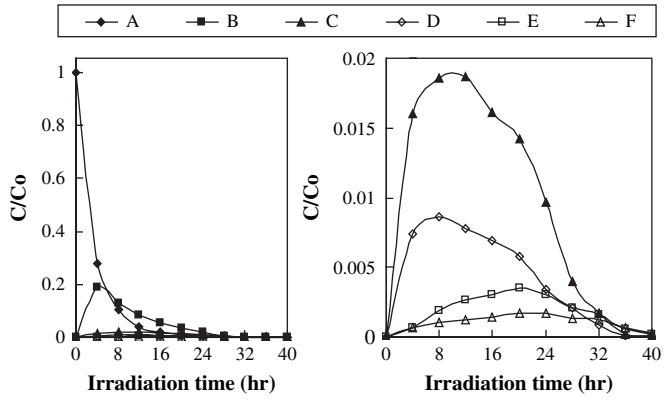

Fig. 9. Variation in the relative distribution of the *N*-de-methylated products obtained from the photodegradation of the AO dye as a function of the irradiation time. Curves A–F correspond to peaks **A**–**F** in Fig. 6, respectively.

events (such as •OH attack, oxygen attack and hydrolysis, or deprotonation) to yield bi-*N*-de-methylated dye derivatives, AO-D and AO-MM. The *N*-de-methylation process as described above continues until formation of the completely *N*-de-methylated dye, AO-DD.

4. Conclusions

AO can be successfully decolorized and degraded by TiO_2 under UV irradiation; after 15-W UV-365 nm irradiation for 24 h, ca. 99.7% of AO was degraded. The photodegradation rate of the dye was found to increase with increasing pH and to increase, and then decrease, with increasing catalyst concentration. Under alkaline conditions, the TiO_2 surface carries a weak negative charge, while AO is primarily positively charged, which will facilitate adsorption and promote photocatalytic degradation. The increase in opacity and light scattering by the TiO_2 particle reduces the degradation rate at high catalyst concentrations. *N*-de-methylation degradation of the dye takes place in a stepwise manner and continues until formation of the completely *N*-de-methylated dye. Methyl groups are removed one by one as confirmed by the gradual

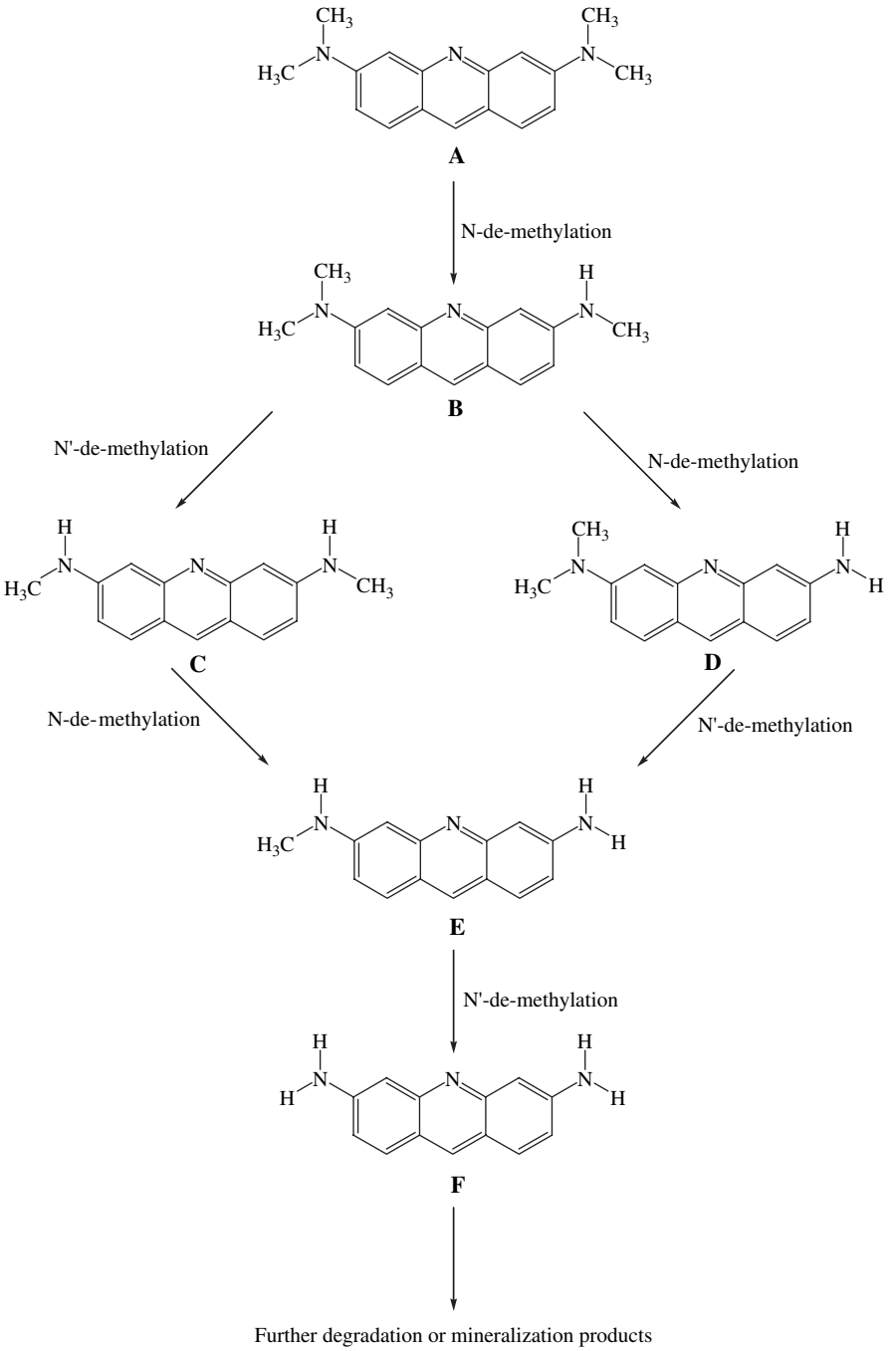

Scheme 1. Proposed *N*-de-methylation mechanism of the AO dye under UV irradiation in aqueous TiO_2 dispersions followed by the identification of several intermediates by HPLC–ESI-MS technique.

wavelength shifts of the maximum peaks toward the blue region. Hypsochromic effects resulting from *N*-de-methylation of AO occur concomitantly during irradiation. The reaction mechanism proposed in this study should shed some light on future applications of the technology to the decoloration of other dyes.

Acknowledgment

This work was supported by NSC 95-2622-M-438-001-CC3 of the National Science Council of the Republic of China.

References

[1] Xie Y, Chen F, He J, Zhao J, Wang H. Photoassisted degradation of dyes in the presence of Fe_3^+ and H_2O_2 under visible irradiation. J Photochem Photobiol A: Chem 2000;136:235–40.
[2] Part A27. Triarylmethane and diarylmethane dyes, Ullmann's encyclopedia of industrial chemistry. 6th ed. New York: Wiley-VCH; 2001.
[3] Faisal M, Tariq MA, Muneer M. Photocatalysed degradation of two selected dyes in UV-irradiated aqueous suspensions of titania. Dyes Pigments 2007;72:233–9.
[4] Peng RY, Fan HJ. Ozonalytic kinetic order of dye decoloration in aqueous solution. Dyes Pigments 2005;67:153–9.
[5] Chen S, Cao G. Study on the photocatalytic reduction of dichromate and photocatalytic oxidation of dichlorvos. Chemosphere 2005;60:1308–15.
[6] Chen CC, Lu CS, Chung YC. Photocatalytic degradation of ethyl violet in aqueous solution mediated by TiO_2 suspensions. J Photochem Photobiol A: Chem 2006;181:120–5.
[7] Konstantinou IK, Albanis TA. TiO_2-assisted photocatalytic degradation of azo dyes in aqueous solution: kinetic and mechanistic investigations: a review. Appl Catal B: Environ 2004;49:1–14.
[8] Kyung H, Lee J, Choi W. Simultaneous and synergistic conversion of dyes and heavy metal ions in aqueous TiO_2 suspensions under visible-light illumination. Environ Sci Technol 2005;39:2376–82.
[9] Měšťánková H, Krýsa J, Jirkovský J, Mailhot G, Bolte M. The influence of Fe(III) speciation on supported TiO_2 efficiency: example of monuron photocatalytic degradation. Appl Catal B: Environ 2005;58:185–91.
[10] Chen C, Li X, Zhao J, Hidaka H, Serpone N. Effect of transition metal ions on the TiO_2-assisted photodegradation of dyes under visible irradiation: a probe for the interfacial electron transfer process and reaction mechanism. J Phys Chem B 2002;106:318–24.
[11] Watanabe N, Horikoshi S, Kawasaki A, Hidaka H, Serpone N. Formation of refractory ring-expanded triazine intermediates during the photocatalyzed mineralization of the endocrine disruptor amitrole and related triazole derivatives at UV-irradiated TiO_2/H_2O interfaces. Environ Sci Technol 2005;39:2320–6.
[12] Dimitrijevic NM, Saponjic ZV, Rabatic BM, Rajh T. Assembly and charge transfer in hybrid TiO_2 architectures using biotin–avidin as a connector. J Am Chem Soc 2005;127:1344–5.
[13] Chen CC, Lu CS, Mai FD, Weng CS. Photooxidative *N*-de-ethylation of anionic triarylmethane dye (sulfan blue) in titanium dioxide dispersions under UV irradiation. J Hazard Mater B 2006;137:1600–7.
[14] Duxbury DF. The photochemistry and photophysics of triphenylmethane dyes in solid and liquid media. Chem Rev 1993;93:381–433.
[15] Hoffman MR, Martin ST, Choi W, Bahnemann DW. Environmental applications of semiconductor photocatalysis. Chem Rev 1995;95:69–96.
[16] Daneshvar N, Salari D, Khataee AR. Photocatalytic degradation of azo dye acid red 14 in water: investigation of the effect of operational parameters. J Photochem Photobiol A: Chem 2003;157:111–6.
[17] Dionysiou DD, Suidan MT, Bekou E, Baudin I, Laîné JM. Effect of ionic strength and hydrogen peroxide on the photocatalytic degradation of 4-chlorobenzoic acid in water. Appl Catal B: Environ 2000;26:153–71.
[18] Da Silva CG, Faria JL. Photochemical and photocatalytic degradation of an azo dye in aqueous solution by UV irradiation. J Photochem Photobiol A: Chem 2003;155:133–43.
[19] Zang Y, Farnood R. Photocatalytic decomposition of methyl *tert*-butyl ether in aqueous slurry of titanium dioxide. Appl Catal B: Environ 2005;57:275–82.
[20] Gao Y, Chen B, Li H, Ma Y. Preparation and characterization of a magnetically separated photocatalyst and its catalytic properties. Mater Chem Phys 2003;80:348–55.
[21] Gao Y, Liu H. Preparation and catalytic property study of a novel kind of suspended photocatalyst of TiO_2-activated carbon immobilized on silicone rubber film. Mater Chem Phys 2005;92:604–8.
[22] Zhu X, Yuan C, Bao Y, Yang J, Wu Y. Photocatalytic degradation of pesticide pyridaben on TiO_2 particles. J Mol Catal A 2005;229:95–105.
[23] Piscopo A, Robert D, Weber JV. Influence of pH and chloride anion on the photocatalytic degradation of organic compounds: Part 1. Effect on the benzamide and *para*-hydroxybenzoic acid in TiO_2 aqueous solution. Appl Catal B: Environ 2001;35:117–24.
[24] Ohtani B, Okugawa Y, Nishimoto S, Kagiya T. Photocatalytic activity of titania powders suspended in aqueous silver nitrate solution: correlation with pH-dependent surface structures. J Phys Chem 1987;91:3550–5.
[25] Kim DH, Anderson MA. Solution factors affecting the photocatalytic and photoelectrocatalytic degradation of formic acid using supported TiO_2 thin films. J Photochem Photobiol A: Chem 1996;94:221–9.
[26] Wong CC, Chu W. The direct photolysis and photocatalytic degradation of alachlor at different TiO_2 and UV sources. Chemosphere 2003;50:981–7.
[27] Wu T, Liu G, Zhao J, Hidaka H, Serpone N. Photoassisted degradation of dye pollutants. V. Self-photosensitized oxidative transformation of rhodamine B under visible light irradiation in aqueous TiO_2 dispersions. J Phys Chem B 1998;102:5845–51.
[28] Zhao J, Wu T, Wu K, Oikawa K, Hidaka H, Serpone N. Photoassisted degradation of dye pollutants. 3. Degradation of the cationic dye rhodamine B in aqueous anionic surfactant/TiO_2 dispersions under visible light irradiation: Evidence for the need of substrate adsorption on TiO_2 particles. Environ Sci Technol 1998;32:2394–400.
[29] Zhao W, Chen C, Li X, Zhao J, Hidaka H, Serpone N. Photodegradation of sulforhodamine-B dye in platinized titania dispersions under visible light irradiation: Influence of platinum as a functional co-catalyst. J Phys Chem B 2002;106:5022–8.
[30] Chen C, Zhao W, Li J, Zhao J, Hidaka H, Serpone N. Formation and identification of intermediates in the visible-light-assisted photodegradation of sulforhodamine-B dye in aqueous TiO_2 dispersion. Environ Sci Technol 2002;36:3604–11.
[31] Liu G, Li X, Zhao J, Hidaka H, Serpone N. Photooxidation pathway of sulforhodamine-B. Dependence on the adsorption mode on TiO_2 exposed to visible light radiation. Environ Sci Technol 2000;34:3982–90.
[32] Bianco PA, Vincenti M, Banciotto A, Pramauro E. Photocatalytic and photolytic transformation of chloramben in aqueous solutions. Appl Catal B: Environ 1999;22:149–58.
[33] Nakamura R, Nakato Y. Primary intermediates of oxygen photoevolution reaction on TiO_2 (rutile) particles, revealed by in situ FTIR absorption and photoluminescence measurements. J Am Chem Soc 2004;126:1290–8.
[34] Murakami Y, Kenji E, Nosaka AY, Nosaka Y. Direct detection of OH radicals diffused to the gas phase from the UV-irradiated photocatalytic TiO_2 surfaces by means of laser-induced fluorescence spectroscopy. J Phys Chem B 2006;110:16808–11.
[35] Galliani G, Rindone B, Scolastico C. Selective de-methylation in the oxidation of arylalkylmethylamines with metal acetates. Tetrahedron Lett 1975;16:1285–8.
[36] Shaefer FC, Zimmermann WD. Dye-sensitized photochemical autooxidation of aliphatic amines in non-aqueous media. J Org Chem 1970;35:2165–74.
[37] Laube BL, Asirvatham MR, Mann CK. Electrochemical oxidation of tropanes. J Org Chem 1977;42:670–4.